



## Study on charge mobility of hexathiapentacene and its selenium analogs

SU-QIN ZHOU<sup>1</sup>, QI-YING XIA<sup>2\*</sup>, MENG LIANG<sup>3</sup> and XUE-HAI JU<sup>3\*\*</sup>

<sup>1</sup>Faculty of Chemical Engineering, Huaiyin Institute of Technology, Key Laboratory for Attapulgite Science and Applied Technology of Jiangsu Province, Huaian 223003, P. R. China, <sup>2</sup>School of Chemistry and Chemical Engineering, Linyi University, Linyi 276005, P. R. China and <sup>3</sup>School of Chemical Engineering, Nanjing University of Science and Technology, Nanjing 210094, P. R. China

(Received 11 May, revised 23 July, accepted 29 July 2020)

**Abstract:** The relationship between molecular geometries, crystal structures and charge mobilities of hexathiapentacene (HTP) and three of its derivatives (2Se-HTP, 4Se-HTP, 6Se-HTP) were studied using the density functional theory combined with a hopping mechanism at the molecular and crystal level. The effect of Se substitution on the charge mobility was discussed. The calculated results showed that the derivatives exhibit good planarity and the molecular geometries show little variation during the charge transfer process. The electron mobility is  $1.20 \text{ cm}^2 \text{ V}^{-1} \text{ S}^{-1}$  for HTP and  $2.30 \text{ cm}^2 \text{ V}^{-1} \text{ S}^{-1}$  for 6Se-HTP, which are much larger than the corresponding hole ones, indicating that HTP and 6Se-HTP are good candidates for *n*-type organic semiconductors. However, 2Se-HTP and 4Se-HTP have comparable hole and electron mobilities and are suitable for ambipolar semiconductors.

**Keywords:** selenium substitution; organic semiconductor; density functional theory; hopping mechanism; ambipolar.

### INTRODUCTION

Over the past decades, organic field effect transistors (OFET) have attracted more and more attention due to their advantages, such as low cost and ease of fabrication on a large scale.<sup>1–4</sup> The charge mobility of OFETs made from some small molecules by the vacuum deposition and solution processing method has already approached that of a polycrystalline silicon field effect transistor, the charge mobility of which is over  $10 \text{ cm}^2 \text{ V}^{-1} \text{ S}^{-1}$ . These OFETs are considered to have promising applications in radio frequency identification devices, organic light-emitting displays and sensor-based equipment.<sup>5</sup> All these potential applications are dependent on high charge mobilities. Therefore, it is still a challenging

\*•\*\* Corresponding authors. E-mail: (\*)xiaqiyi@163.com; (\*\*)xhju@njust.edu.cn  
<https://doi.org/10.2298/JSC200511045Z>

task in the field of organic electronics to design and fabricate new organic semiconductors with high charge mobility, ease of storage, and stable to handle.

The electronic property, solubility and molecular packing in organic semiconductors could be regulated and controlled by the introduction of heteroatoms, such as halogens, sulfur and nitrogen atoms.<sup>6,7</sup> Among the heteroatoms in organic semiconductors, selenium is not as common as sulfur and nitrogen. The available investigations showed that the effects of sulfur being replaced by selenium are not really uniform. The difference in charge mobilities between tetra-thiofuran and selenium-substituted tetrathiofuran is almost neglectable.<sup>8</sup> However, the charge mobility increases noticeably from 0.081 to 0.17 cm<sup>2</sup> V<sup>-1</sup> S<sup>-1</sup> in DNTT/DNSS when the sulfur atoms of the latter are replaced by selenium.<sup>9</sup> In 2011, Lee and coworkers reported a series of metal chalcogenides of cadmium selenide nanocrystals and their charge transferring. The electron mobility was up to 16 cm<sup>2</sup> V<sup>-1</sup> S<sup>-1</sup>,<sup>10</sup> a value that is greater than that of the best dissolved organic nanocrystalline devices by one order of magnitude. In a word, the selenium compounds used in organic semiconductors are not as popular as sulfur- or nitrogen-containing compounds. The replacement of sulfur by selenium is an appropriate strategy to develop high-performance organic semiconductor materials.<sup>11</sup>

In 2006, Briseno and his colleagues studied the molecular structure, molecular packing of hexathiapentacene (HTP) and its application in light-emitting diodes.<sup>12,13</sup> Both face to face  $\pi$ - $\pi$  interaction and S···S interaction contribute to the charge transfer. Since sulfur and selenium belong to the same group and the latter has more d-electrons, the replacement of sulfur with selenium is expected to improve the charge transfer property. To probe the influence of selenium substitution, the molecular and crystal structures, and charge mobilities of HTP and its selenium analogs (Fig. 1) were studied by the density functional theory method together with the charge carrier hopping model.

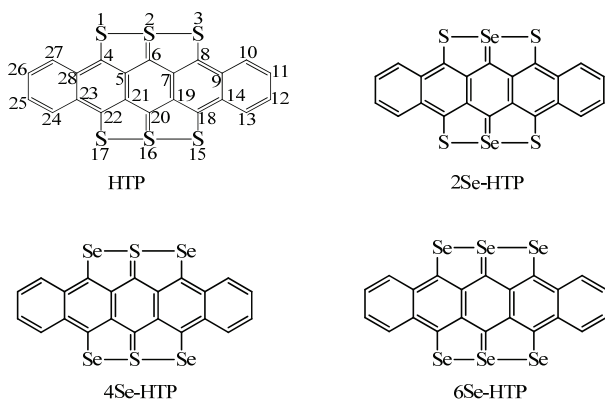


Fig. 1. Molecular structure and atomic numbering of HTP and its analogs with the same atomic numbering.

## EXPERIMENTAL

The hybrid functional of B3LYP was proved to be appropriate for organic molecules with  $\pi$  conjugations.<sup>14</sup> Therefore, the reorganization energy in the charge transfer process was obtained at the B3LYP/6-311++G\*\* level. Consequently, the optimized geometrical structures of the neutral molecules and the ionization energy, electron affinity, and energies of HOMO and LUMO of the corresponding cations and anions were calculated. Whereas, the PW91PW91/6-31G(d) was used for the molecular packing of the dimers and the charge transfer integral, since computational practice showed that this method produces rational results for the coupling integral.<sup>15-16</sup> All the above-mentioned quantum calculations were performed by the Gaussian 09 package.<sup>17</sup>

The crystal structure of HTP is from Cambridge Crystal Database. Both the crystal and molecular structure were optimized by the DFT-D method with PBE functionals. The dispersion corrected method (-D) has commonly been used to describe weak interactions.<sup>18</sup> As displayed in Table I, the optimized cell parameters are in good agreement with the experimental values, indicating the DFT-D method and the basis set used could be adopted for the system. Since sulfur and selenium are in the same group, it is reasonable to use the same method for predicting the crystal structures of the selenium analogs when the sulfur is substituted by selenium.<sup>19</sup> The calculations for the crystals were performed by the CASTEP module.<sup>20</sup>

According to the incoherent hopping mechanism, the charge carriers localize and jump between neighboring molecules to migrate across the organic layer.<sup>21</sup> The charge transfer rate between neighboring molecules is:

$$k_i = \frac{2\pi t_i^2}{h} \left( \frac{\pi}{\lambda_- k_B T} \right)^{0.5} \exp\left(-\frac{\lambda_-}{4k_B T}\right) \quad (1)$$

where  $t_i$  is the transfer integral between neighboring molecules in each individual hopping pathway, and  $\lambda_-$  is the reorganization energy for electron transports,  $T$  is the temperature,  $h$  and  $k_B$  are the Planck and Boltzmann constants, respectively. The charge coupling  $t_i$  was calculated by considering the spatial overlap between two monomers according to:<sup>22</sup>

$$t_i = \frac{h_{12} - 0.5(h_{11} + h_{22})S_{12}}{1 - S_{12}^2} \quad (2)$$

where  $h_{ij}$  is the charge transfer integral and  $S_{ij}$  is the spatial overlap integral. The charge transfer mobility is evaluated by the Einstein Relation:

$$\mu = \frac{e}{k_B T} D \quad (3)$$

where  $e$  is the electron charge,  $k_B$  Boltzmann constant, and  $D$  diffusion coefficient that is a sum along the  $i^{\text{th}}$  hopping pathway:<sup>23</sup>

$$D = \frac{1}{2n} \sum_i r_i^2 k_i P_i \quad (4)$$

where  $n$  is the space dimensionality,  $r_i$  is the centroid distance of the hopping channel  $i$ ,  $k_i$  is the hopping rate in the  $i$  pathway, and  $P_i$  is the relative probability for charge carrier hopping determined by:

$$P_i = \frac{k_i}{\sum_i k_i} \quad (5)$$

## RESULTS AND DISCUSSION

### *Geometrical structures*

The optimized bond lengths of HTP are in good agreement with the single crystal X-ray diffraction structure (Table I), indicating that the B3LYP/6-311++G\*\* method is appropriate for HTP. The changes of the bond lengths from molecule to anion  $\Delta(A-G)$  and to cation  $\Delta(C-G)$  are shown in Figs. S-2 and S-3 of the Supplementary material to this paper, respectively. The maximum variations of bond lengths are 0.023 Å for HTP and 2Se-HTP, and 0.024 Å for 4Se-HTP and 6Se-HTP, indicating the variation of structure is small upon the molecule donating or accepting an electron. This is beneficial for the charge transfer. As seen in Figs. S-2 and S-3, the lengths of 1 to 3, 25 to 29 bonds, and bonds associated with labels 35 and 36 vary largely from molecule to anion. The bond lengths associated with labels 3, 13, 25, 29, 33 and 35 vary largely from molecule to cation. These bonds with large length variations are C–S, C–Se, S–S and Se–Se, indicating these atoms make large contributions to the charge transfer.

TABLE I. Experimental and calculated cell parameters of HTP and its selenium analogs

Compound	$\alpha / {}^\circ$	$\beta / {}^\circ$	$\gamma / {}^\circ$	$a / \text{\AA}$	$b / \text{\AA}$	$c / \text{\AA}$
HTP <sup>a</sup>	72.46	88.89	84.17	3.894	14.33	16.55
HTP <sup>b</sup>	73.43	88.73	82.08	3.837	14.22	16.64
2Se-HTP	75.55	89.65	88.29	3.872	13.14	17.44
4Se-HTP	73.55	88.85	82.53	3.893	14.33	16.58
6Se-HTP	75.05	89.15	84.65	3.918	13.42	17.43

<sup>a</sup>Experimental values from the Cambridge Crystal Database; <sup>b</sup>This work

### *Frontier molecular orbitals*

The electronic structures and energies of frontier molecular orbitals greatly influence charge transfer.<sup>24</sup> As seen from the contours of Fig. 2, the HOMO is symmetric, while the LUMO is asymmetric. The contours of HOMO distribute on almost all heavy atoms (non-hydrogen atoms) except for S or Se, while those of LUMO are on all heavy atoms. The delocalized distribution is favorable for electron transfer. The energies of HOMO and LUMO determine the injection of a hole and electron. A low LUMO is beneficial for the injection of electrons.<sup>25</sup> The energy difference ( $E_{\text{gap}}$ ) between HOMO and LUMO is also an important factor for the injection of charge. A small  $E_{\text{gap}}$  value is beneficial for charge injection.<sup>26</sup> As seen in Table II, the  $E_{\text{gap}}$  values for 4Se-HTP and 6Se-HTP are relatively small, indicating that these compounds are adequate for *n*-type OSC.

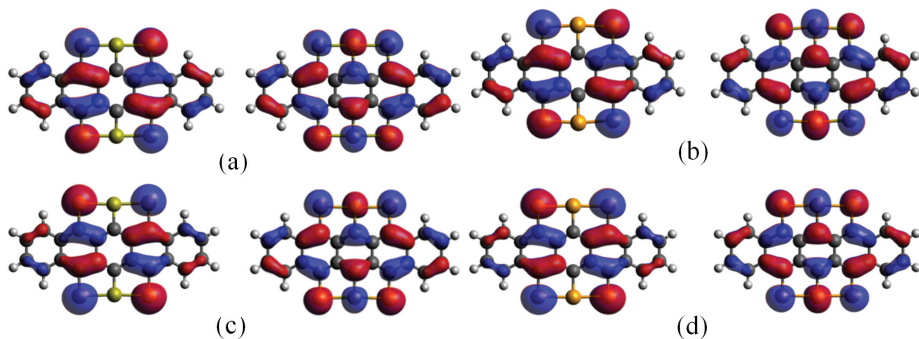


Fig. 2. Contours of LUMO (left) and HOMO (right) for HTP (a), 2Se-HTP (b), 4Se-HTP (c) and 6Se-HTP (d).

TABLE II. Energies of HOMO and LUMO, and their gap

Compound	$E_{\text{HOMO}} / \text{eV}$	$E_{\text{LUMO}} / \text{eV}$	$E_{\text{gap}} / \text{eV}$
HTP	-5.27	-3.51	1.76
2Se-HTP	-5.28	-3.48	1.80
4Se-HTP	-5.20	-3.52	1.68
6Se-HTP	-5.23	-3.50	1.73

#### *Electron affinity, ionization energy and reorganization energy*

The ionization energy, electron affinity and reorganization energy are listed in Table III. For a good electron injection, the electron affinity should be large enough. Similarly, a small ionization energy is favorable for hole transfer. After Se substitution, the ionization energy decreases, but the electron affinity increases excepted for 2Se-HTP, indicating the substitution of Se improves the hole and electron transfer.

TABLE III. Ionization potential ( $IP$ ), electron affinity ( $EA$ ) and reorganization energy ( $\lambda_e$  for electron and  $\lambda_h$  for hole) at the B3LYP/6-311++G\*\* level; subscripts “v” and “a”, following IP and EA, denote the corresponding vertical and adiabatic values

Compound	$IP_v / \text{eV}$	$IP_a / \text{eV}$	$EA_v / \text{eV}$	$EA_a / \text{eV}$	$\lambda_e / \text{eV}$	$\lambda_h / \text{eV}$
HTP	6.78	6.72	2.30	2.37	0.145	0.137
2Se-HTP	6.79	6.72	2.28	2.35	0.139	0.142
4Se-HTP	6.72	6.66	2.37	2.43	0.133	0.110
6Se-HTP	6.73	6.68	2.36	2.42	0.128	0.114

As one of the key factors for charge transfer, the reorganization energy is related to the molecular size and geometrical structure. Generally speaking, the larger the deformation is during charge transfer, the larger is the reorganization energy, and the smaller is the charge transfer rate. By summing up the absolute values of bond length variations (denoted as  $\sum|\Delta r_{A-G}|$  and  $\sum|\Delta r_{C-G}|$ ) of anion/molecule and cation/molecule (Tables S-1–S-4), it could be found that the values

of  $\sum |\Delta r_{C-G}|$  are in the order: 2Se-HTP > HTP > 6Se-HTP > 4Se-HTP, which is in accordance with the order of the hole reorganization energy ( $\lambda_h$ ). For electron transfer, the reorganization energy decreases after Se substitution, indicating Se substitution favors electron transfer.

#### *Charge transfer integral and charge mobility*

The charge transfer integral is closely related to the molecular packing and center-of-mass distance of neighboring molecules. The space group of the crystal is supposed to be similar when S is replaced by Se since both the elements have almost the same electronegativity (2.58 vs. 2.55) and thereby similar intermolecular force. As seen in Fig. 3, the molecules in HTP and its selenium analogs are packed in fishbone patterns after geometrical and cell parameter optimization. The dimers in hopping paths of P1 and P2 are in face-to-face  $\pi-\pi$  packing, which is proved by many literature references to be an efficient packing for charge hopping.<sup>27</sup>

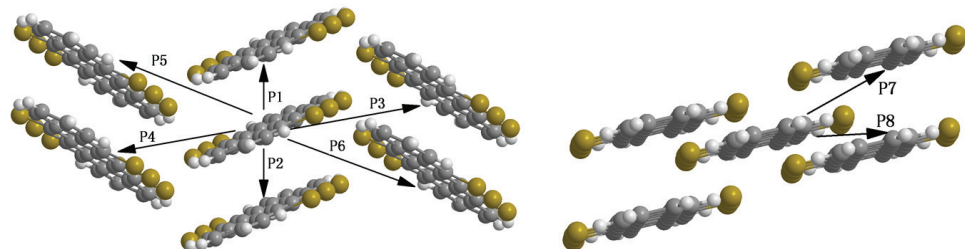


Fig. 3. Paths for charge hopping.

The charge transfer integrals in P1 and P2 hopping are the largest for both hole and electron transfer. As seen in Table IV, the maximum absolute values of charge transfer integrals for electron hopping are 37.3, 37.1, 53.4 and 55.1 meV for HTP, 2Se-HTP, 4Se-HTP and 6Se-HTP, respectively. Those for hole hopping are 101.9, 61.0, 123.2 and 119.3 meV, respectively. Moreover, the larger the center-of-mass distance is, the smaller is the overlap integral between the orbitals of neighboring molecules. The intermolecular orbital interaction will vanish, and the charge transfer integral will become zero when the center-of-mass distance exceeds a certain value. For example, the center-of-mass distance  $r_i$  is 3.84 Å in dimer P1 of HTP and the corresponding hole transfer integral is 101.9 meV. The center-of-mass distance in P3 (12.72 Å) is three times larger than in P1 and its transfer integral is only one fiftieth of the latter. While the center-of-mass distance in P8 is 15.23 Å and the transfer integral is nearly zero. In view of charge transfer integral, 4Se-HTP possess the maximum hole transfer integral and is a candidate for *p*-type OSC. 6Se-HTP has the maximum electron transfer integral and is a promising candidate for *n*-type OSC.

TABLE IV. Charge transfer integral ( $h_e$  for electron and  $h_h$  for hole) for neighboring molecule dimer; charge transfer integral at the PW91PW91/6-31G (d, p) level;  $S$  is the overlap matrix of the dimer

Compound	Path <sup>a</sup>	$h_e$ / meV	$S_e^{ij}$	$h_h$ / meV	$S_h^{ij}$	$r^b$ / Å
HTP	1	37.3	-0.0065	101.9	-0.0201	3.84
	2	-37.1	0.0065	101.8	-0.0201	3.84
	3	-4.1	0.0004	2.5	-0.0003	12.72
	4	-4.3	0.0009	-1.7	0.0004	9.31
	5	-0.7	0.0003	3.0	-0.0004	9.63
	6	-5.1	0.0006	3.0	-0.0004	12.36
	7	-1.0	0.0001	0.6	-0.0001	14.22
	8	1.9	-0.0002	0.8	-0.0001	15.23
2Se-HTP	1	31.7	-0.0059	61.0	-0.013	3.87
	2	-31.7	0.0059	61.0	-0.013	3.87
	3	5.1	-0.0005	-3.1	0.0003	0.99
	4	-3.0	0.0004	-10.8	0.0019	0.99
	5	3	-0.0004	-10.5	0.0018	0.99
	6	-5.5	0.0006	-3.3	0.0004	0.99
	7	-1.3	0.0001	-1.0	0.000	6.21
	8	6.9	-0.0008	4.7	-0.0005	6.21
4Se-HTP	1	-53.4	0.0093	123.2	-0.024	3.89
	2	-53.4	0.0093	123.1	-0.024	3.89
	3	-4.4	0.001	-6.1	0.0011	0.62
	4	-4.4	0.0004	2.5	-0.0003	0.62
	5	-7.1	0.0008	3.9	-0.0005	0.62
	6	0.6	0.0002	3.9	-0.0004	0.62
	7	-0.6	0.0001	0.3	0.000	14.33
	8	0.7	-0.0001	-1.6	0.0002	15.33
6Se-HTP	1	-55.1	0.0096	119.3	-0.0228	3.92
	2	55.1	-0.0096	119.3	-0.0228	3.92
	3	4.8	-0.0005	2.9	-0.0003	12.57
	4	0.1	0.000	13.3	-0.0022	9.63
	5	1.3	-0.0002	12.1	-0.002	9.83
	6	6.5	-0.0007	3.7	-0.0004	12.33
	7	1.1	-0.0001	-0.5	0.000	13.42
	8	3.4	-0.0004	1.9	-0.0002	14.33

<sup>a</sup>See Fig. 3 for paths; <sup>b</sup>center-of-mass distance of neighboring monomers

As seen in Table V, the electron mobility is  $1.20 \text{ cm}^2 \text{ V}^{-1} \text{ S}^{-1}$  for HTP and  $2.30 \text{ cm}^2 \text{ V}^{-1} \text{ S}^{-1}$  for 6Se-HTP, which are much larger than their corresponding hole ones, indicating that HTP and 6Se-HTP are good candidates for *n*-type organic semiconductors. However, 2Se-HTP and 4Se-HTP have comparative hole and electron mobilities and are suitable for ambipolar semiconductors.

TABLE V. Hole and electron mobilities

Comp.	$\mu_h$ / $\text{cm}^2 \text{ V}^{-1} \text{ s}^{-1}$	$\mu_e$ / $\text{cm}^2 \text{ V}^{-1} \text{ s}^{-1}$	Comp.	$\mu_h$ / $\text{cm}^2 \text{ V}^{-1} \text{ s}^{-1}$	$\mu_e$ / $\text{cm}^2 \text{ V}^{-1} \text{ s}^{-1}$
HTP	0.14	1.2	4Se-HTP	0.61	0.92
2Se-HTP	0.19	0.28	6Se-HTP	0.41	2.29

## CONCLUSIONS

The charge transfer features of HTP and its selenium analogs were investigated by DFT and the charge carrier hopping mechanism. The stabilities of the selenium analogs are increased, and the reorganization energies decreased compared to the parent those of HTP. In view of the contours and energies of the frontier molecular orbitals, HTP and its selenium analogs are suitable for *n*-type OSCs. 4Se-HTP and 6Se-HTP have lower LUMO and  $E_{gap}$ , which is more favorable for electron injection. The face-to-face  $\pi-\pi$  packing of HTP and its selenium analogs guarantees large charge transfer integrals and is thus beneficial for charge transfer. Both the electron mobilities of HTP and 6Se-HTP are larger than the hole ones, and HTP and 6Se-HTP are adopted for *n*-type OSCs. 2Se-HTP and 4Se-HTP have the similar magnitudes of electron and hole mobilities and are thus candidates for bipolar OSCs. The present study showed that selenium substitution for sulfur is one of the strategies to develop *n*-type or ambipolar semiconductors.

## SUPPLEMENTARY MATERIAL

Additional data are available electronically at the pages of journal website: <https://www.shd-pub.org.rs/index.php/JSCS/index>, or from the corresponding author on request.

*Acknowledgement.* The authors thank the National Science Foundation of China (No. 21372116) for supporting this work.

ИЗВОД  
ТЕОРИЈСКО ПРОУЧАВАЊЕ ПОКРЕТЉИВОСТИ НАЕЛЕКТРИСАЊА КОД  
ХЕКСАТИОПЕНТАЦЕНА И ЊЕГОВИХ СЕЛЕНОВИХ АНАЛОГА

SU-QIN ZHOU<sup>1</sup>, QI-YING XIA<sup>2</sup>, MENG LIANG<sup>3</sup> и XUE-HAI JU<sup>3</sup>

<sup>1</sup>*Faculty of Chemical Engineering, Huaiyin Institute of Technology, Key Laboratory for Attapulgite Science and Applied Technology of Jiangsu Province, Huai'an 223003, P. R. China*, <sup>2</sup>*School of Chemistry and Chemical Engineering, Linyi University, Linyi 276005, P. R. China* и <sup>3</sup>*School of Chemical Engineering, Nanjing University of Science and Technology, Nanjing 210094, P. R. China*

Теоријом функционала густине комбинованом са механизmom прескацања проучаван је однос између молекулских геометрија, кристалних структуре и покретљивости наелектрисања у хексатиопентацена (HTP) и његова три деривата (2Se-HTP, 4Se-HTP, 6Se-HTP) на нивоу молекула и кристала. Дискутован је ефекат супституције селеном на покретљивост наелектрисања. Израчунати резултати показују да деривати имају добру планарност и да геометрије молекула мало варирају током процеса преноса наелектрисања. Мобилност електрона је  $1,20 \text{ cm}^2 \text{ V}^{-1} \text{ S}^{-1}$  за HTP и  $2,30 \text{ cm}^2 \text{ V}^{-1} \text{ S}^{-1}$  за 6Se-HTP, што је много веће него за одговарајуће празнине, указујући да су HTP и 6Se-HTP добри кандидати за органске полупроводнике *n*-типа. Међутим, 2Se-HTP и 4Se-HTP имају упоредиве покретљивости електрона и шупљина и погодни су за амбиполарне полупроводнике.

(Примљено 11. маја, ревидирано 23. јула, прихваћено 29. јула 2020)

## REFERENCES

1. H. Usta, A. Facchetti, T. J. Marks, *Acc. Chem. Res.* **44** (2011) 501 (<https://dx.doi.org/10.1021/ar200006r>)
2. X. Wang, K. C. Lau, *J. Phys. Chem., C* **116** (2012) 22749 (<https://dx.doi.org/10.1021/jp309226z>)
3. A. Datta and S. K. Pati, *J. Phys. Chem., C* **111** (2007) 4487 (<https://dx.doi.org/10.1021/jp070609n>)
4. N. Z. Prlainovic, M. P. Rancic, I. Stojiljkovic, J. B. Nikolic, S. Z. Drmanic, I. Ajaj, A. D. Marinkovic, *J. Serb. Chem. Soc.* **83** (2018) 139 (<https://doi.org/10.2298/JSC170408003P>)
5. A. Tripathi, C. Prabhakar, *J. Chin. Chem. Soc.* **65** (2018) 918 (<https://dx.doi.org/10.1002/jccs.201700448>)
6. Y. Song, C. Di, X. Yang, *J. Am. Chem. Soc.* **128** (2007) 15940 (<https://dx.doi.org/10.1021/ja064726s>)
7. M. Melucci, L. Favaretto, M. Zambianchi, *Chem. Mater.* **25** (2013) 668 (<https://dx.doi.org/10.1021/cm303224a>)
8. H. W. Lin, W. Y. Lee, C. Lu, *Polym. Chem.* **3** (2012) 767 (<https://dx.doi.org/10.1039/c2py00583b>)
9. T. Yamamoto, K. Takimiya, *J. Am. Chem. Soc.* **129** (2007) 2224 (<https://dx.doi.org/10.1021/ja068429z>)
10. A. L. Briseno, S. C. B. Mannsfeld, E. Formo, *J. Mater. Chem.* **18** (2008) 5395 (<https://dx.doi.org/10.1039/b809228c>)
11. A. Bedi, S. P. Senanayak, K. S. Narayan, S. S. Zade, *Macromolecules* **46** (2013) 5943 (<https://dx.doi.org/10.1021/ma4008219>)
12. A. L. Briseno, S. C. B. Mannsfeld, X. Lu, Y. Xiong, S. A. Jenekhe, Z. Bao, Y. Xia, *Nano Lett.* **7** (2007) 668 (<https://dx.doi.org/10.1021/nl0627036>)
13. A. L. Briseno, Q. Miao, M. M. Ling, *J. Am. Chem. Soc.* **128** (2007) 15576 (<https://dx.doi.org/10.1021/ja066088j>)
14. K. Chaitanya, X. H. Ju, B. M. Heron, *RSC Adv.* **5** (2015) 3978 (<https://dx.doi.org/10.1039/c4ra09914a>)
15. O. Castellano, R. Gimon, H. Soscul, *Energy Fuel* **25** (2011) 2526 (<https://dx.doi.org/10.1021/ef101471t>)
16. Y. Hong, Y. R. Liu, H. Wen, *RSC Adv.* **8** (2018) 7225 (<https://dx.doi.org/10.1039/c7ra13670f>)
17. *Gaussian 09*, Revision A.02, Gaussian, Inc., Wallingford, CT, 2009
18. A. Krishtal, K. Vannomeslaeghe, A. Olasz, *J. Chem. Phys.* **130** (2009) 174101 (<https://dx.doi.org/10.1063/1.3126248>)
19. Y. Hu, K. Chaitanya, J. Yin, X. H. Ju, *J. Mater. Sci.* **51** (2016) 6235 (<https://dx.doi.org/10.1007/s10853-016-9921-8>)
20. M. D. Segall, P. L. D. Lindan, M. J. Probert, C. J. Pickard, P. J. Hasnip, S. J. Clark, M. C. Payne, *J. Phys.: Cond. Matt.* **14** (2002) 2717 (<https://dx.doi.org/10.1088/0953-8984/14/11/301>)
21. M. D. Hanwell, T. A. Madison, G. R. Hutchison, *J. Phys. Chem., C* **114** (2010) 20417 (<https://dx.doi.org/10.1021/jp104416a>)
22. S. Mohakud, A. P. Andrews, S. K. Pati, *J. Phys. Chem., C* **114** (2010) 20436 (<https://dx.doi.org/10.1021/jp1047503>)
23. W. Q. Deng and W. A. Goddard III, *J. Phys. Chem., B* **108** (2004) 8614 (<https://dx.doi.org/10.1021/jp0495848>)

24. J. Yin, K. Chaitanya, X. H. Ju, *RSC Adv.* **5** (2015) 65192 (<https://dx.doi.org/10.1039/C5RA06418J>)
25. J. M. Hancock, A. P. Gifford, R. D. Champion, *Macromolecules* **41** (2008) 3588 (<https://dx.doi.org/10.1021/ma800304m>)
26. J. Yin, K. Chaitanya, X. H. Ju, *Can. J. Chem.* **93** (2015) 740 (<https://dx.doi.org/10.1139/cjc-2014-0569>)
27. M. Liang, J. Yin, K. Chaitanya, X. H. Ju, *J. Theor. Comput. Chem.* **15** (2016) 1650027 (<https://dx.doi.org/10.1142/S0219633616500279>).